

Removal of Copper Ions from Wastewater by Adsorption onto a Green Adsorbent from Winemaking Wastes

Lorena Alcaraz, Irene García-Díaz, Francisco J. Alguacil, and Felix A. López *

Copper ion adsorption was studied using an activated carbon from winemaking wastes. The pH, temperature, activated carbon amount, and initial copper concentration were varied based on a full factorial 2^k experimental design. Kinetic and thermodynamic studies were also performed. The adsorption kinetics followed a pseudo-second-order model. The adsorption data fit best to the Langmuir isotherm, compared with the Freundlich and Temkin models. The analysis of variance demonstrated that the pH and the activated carbon dosage had the greatest influences on the copper adsorption. The obtained activation energy suggested that the copper adsorption was physisorption. The best fit to a linear correlation was the moving boundary equation, which controls the kinetics of the adsorption of copper ions onto the activated carbon. X-ray photoelectron spectroscopy revealed the existence of different copper species (Cu^{2+} , and Cu^+ and/or Cu^0) on the surface of the carbonaceous adsorbent after the adsorption, which could suggest a simultaneous reduction process.

Keywords: Activated carbon; Adsorption; Copper; Winemaking wastes

Contact information: National Center for Metallurgical Research (CENIM). Spanish National Research Council (CSIC), Avda. Gregorio del Amo, 8, 28040 Madrid, Spain;

* *Corresponding author:* f.lopez@csic.es

INTRODUCTION

The contamination of water by toxic heavy metals is a worldwide environmental problem that has increasingly focused the attention of the scientific community (Demiral and Güngör 2016). Heavy metals such as Cu, Cd, Pb, and Zn, among others, are present in water through the discharge of industrial wastewater and are toxic to humans and other living species when their concentrations exceed certain values (Aydın *et al.* 2008). In humans, poisoning by copper ingestion may show systemic effects such as hemolysis or liver and kidney damage. In addition, other local effects have been reported, such as irritation of the upper respiratory tract, gastrointestinal disturbance with vomiting and diarrhea, and a form of contact dermatitis (Demiral and Güngör 2016). Moreover, these heavy metals exhibit a great potential to inhibit the growth of various aquatic plants and microorganisms (Li *et al.* 2018; Zhou *et al.* 2019). All of these effects contribute to the necessity of treating copper-containing wastewater (Feng *et al.* 2009). The U. S. Environmental Protection Agency (EPA) has set a guidance level for copper in drinking water at 1.3 mg/L (Sudha Rani *et al.* 2018).

Copper ions may be present in water *via* several sources, such as mining operations, machinery, electric power, chemical industry, electroplating processes, petroleum refining, or pesticide industries (Ferreira da Silva *et al.* 2018). For copper removal, different methods have been studied, such as precipitation (Coudert *et al.* 2013), ion exchange (Caprarescu *et al.* 2009; Modrogan *et al.* 2013, 2015; Ntimbani *et al.* 2015),

membrane filtration (Caprarescu *et al.* 2014; Kalaiselvi *et al.* 2015), electro dialysis (Caprarescu *et al.* 2015), and ionic flocculation (Carvalho Barros *et al.* 2018). However, these removal methods for heavy metal have some disadvantages, such as its high cost, the incomplete removal of the contaminant or the possible of secondary contamination on the production, among others (Feng *et al.* 2009; He *et al.* 2018). Recently, adsorption method has been shown to have advantages over other methods for heavy metal removal (high efficiency, low cost, and easy operation has been widely applied). Adsorptive removal of heavy metal ions from aqueous solutions by a low-cost adsorbent (which is defined as a material that is abundant in nature or is a by-product or waste material from industry) such as bioadsorbents (He *et al.* 2018; Sajjadi *et al.* 2018; Saleh *et al.* 2018; Wu *et al.* 2019) and activated carbon obtained from biomass (Alguacil *et al.* 2018; Alcaraz *et al.* 2019; Liu *et al.* 2020) is a constant research subject.

Activated carbons (ACs) are known as very effective adsorbents. They are characterized by high porosity, great surface area, variable characteristics of surface chemistry, and a high degree of surface reactivity (Hu and Srinivasan 1999; Alcaraz *et al.* 2018). However, ACs have high production costs and are usually more expensive than other types of adsorbents. Consequently, the production of ACs from renewable and cheaper precursors has recently attracted growing attention from researchers (Liew *et al.* 2019; Yek *et al.* 2019). In recent years, ACs from different wastes, such as barley straw (Pallarés *et al.* 2018), pistachio wood (Sajjadi *et al.* 2018), coconut shells (Yang *et al.* 2010), wild olive cores (Kaouah *et al.* 2013), and winemaking waste (Alguacil *et al.* 2018), have been tested as effective candidates for adsorptive metal removal.

In this sense, due to a lot of generated wastes from winemaking (cultivation harvesting about 5 tonnes ha⁻¹ per year (leaves and canes, *etc.*), while the produced waste by winemaking process may reach 25% of that of the grapes used), it is necessary ways of dealing with this waste have been sought (Alcaraz *et al.* 2018). For this reason, a successful process that involves both a generation of a green adsorbent from winemaking wastes and the metal removal from waterwastes is of great interest to the scientific community.

This study obtained and characterized AC from a winemaking waste, bagasse. Experiments were performed that modified the pH value, the copper concentration, the adsorbent dosage, and the temperature to investigate the adsorbent capacity of copper ions on the AC. The results were analyzed by a statistical experimental design, and the influences of three factors were considered: solution pH, metal concentration, and adsorbent dosage.

EXPERIMENTAL

Materials

Activated carbon from a winemaking waste, bagasse, was obtained as follows (Alcaraz *et al.* 2018; Alguacil *et al.* 2018): An aqueous suspension of bagasse waste (75 g/L), from the production of Albariño wine (Denomination of Origin Rías Baixas, Galicia, Spain) and supplied by the Misión Biológica de Galicia (CSIC, Spanish National Research Council) (Pontevedra, Spain), was introduced into a Berghof BR-300 high pressure reactor (Berghof Products + Instruments GmbH, Eningen, Germany) at 523 K and 30 bar for 3 h. The obtained mixture was filtered to separate the generated hydrothermal carbon (HTC), which was dried. An HTC/KOH (potassium hydroxide,

powder, Merck KGaA) (weight ratio 1:2) mixture was introduced at 1073 K for 2 h in a Carbolite STF 15 tube furnace (Carbolite Gero, Hope Valley, UK) under a N₂ atmosphere (150 mL/min) to generate the AC. After cooling to room temperature, the AC was washed with Milli-Q water until reaching a pH of approximately 5. Finally, the AC was dried at 353 K.

Methods

Batch adsorption experiments

The metal adsorption by the activated carbon was performed *via* batch experiments. The temperature was controlled using a Selecta Termotronic thermostat-controlled bath (J.P. Selecta, Barcelona, Spain) equipped with multiple Lab Companion MS-52M stirrers (Jeio Tech, Daejeon, South Korea) until equilibrium was reached. The stirring speed was constant for all adsorption experiments, at 500 revolutions per minute (rpm). One mL of sample was collected at 0 min, 5 min, 10 min, 20 min, 30 min, 40 min, 50 min, 60 min, 120 min, and 180 min and filtered through syringe filters with 0.22- μ m pores and 13-mm diameters.

Copper content (copper II sulphate 5-hydrate, Panreac) in the solution was analyzed by atomic absorption spectroscopy (AAS), and the copper content in the carbon was estimated by mass balance. The pH values of the solutions were adjusted using a pH meter (Sension+ MM340 MultiMeter, Hach Lange Spain S. L. U.) and by adding HCl (0.1 M). The adsorption capacity (q_e) (mg/g) was calculated according to Eq. 1,

$$q_e = \frac{(C_0 - C_e) \cdot V}{m} \quad (1)$$

where C_0 (mg/L) is the initial concentration of copper in solution, C_e (mg/L) is the copper concentration at equilibrium, q_e (mg/g) is the amount of copper adsorbed on the AC at equilibrium, V (L) is the volume of the solution, and m (g) is the mass of the AC.

The equilibrium adsorption isotherm data were plotted using the Langmuir (Eq. 2), Freundlich (Eq. 3), and Temkin (Eq. 4) linear equation models (Aljeboree *et al.* 2017),

$$\frac{C_e}{q_e} = \frac{1}{q_m \cdot b} + \frac{1}{q_m} \cdot C_e \quad (2)$$

$$\ln q_e = \ln K_F + \frac{1}{n} \cdot \ln C_e \quad (3)$$

$$q_e = B \cdot \ln A_T + B \cdot \ln C_e \quad (4)$$

where q_e (mg/g) is the adsorbed metal amount by mass of AC at equilibrium, K_F (L/g) is the Freundlich constant, $1/n$ indicates the intensity of adsorption, q_m (mg/g) is the maximum adsorption capacity of the adsorbent per unit mass of adsorbate, b (L/mg) is the Langmuir constant related to the adsorption energy, C_e (mg/L) is the metal concentration at equilibrium, A_T is the Temkin isotherm equilibrium binding constant (L/g), and $B = R \cdot T / b_T$ is a constant related to the heat of sorption (J/mol), where b_T is the Temkin isotherm constant, R is the universal gas constant (8.314 J/(mol·K)), and T (K) is the absolute temperature. The dimensionless Langmuir constant, or equilibrium parameter, (R_L) indicates if the isotherm is irreversible ($R_L = 0$), favorable ($0 < R_L < 1$), linear ($R_L = 1$), or unfavorable ($R_L > 1$), where $R_L = 1 / (1 + b \cdot C_0)$.

The batch kinetics experiments for copper adsorption on AC were performed at different temperatures and were analyzed using the pseudo-first-order (Eq. 5) (Lagergren 1898) and pseudo-second-order (Eq. 6) (Ho and McKay 1999) kinetic models:

$$\ln(q_e - q_t) = \ln q_e - K_1 \cdot t \quad (5)$$

$$\frac{t}{q_t} = \frac{1}{K_2 \cdot q_e^2} + \frac{1}{q_e} \cdot t \quad (6)$$

where q_t (mg/g) is the adsorbed metal amount per mass of AC at specified contact times (t) (min), q_e (mg/g) is the adsorbed metal amount per mass of AC after equilibration, and K_1 (min^{-1}) and K_2 ($\text{g}/\text{min} \cdot \text{mg}$) are the first-order and second-order adsorption constants, respectively.

Thermal parameters were calculated from Eqs. 7 and 8. The enthalpy change (ΔH° , J/molK) and entropy change (ΔS° , KJ/mol) were calculated from the slope and intercept of a plot of $\log(q_e/C_e)$ versus $1/T$ according to Eq. 7 (Fouodjouo *et al.* 2017),

$$\log \frac{q_e}{C_e} = \frac{\Delta S^\circ}{2.303R} + \frac{\Delta H^\circ}{2.303RT} \quad (7)$$

$$\Delta G^\circ = \Delta H^\circ - T\Delta S^\circ \quad (8)$$

where R is the universal gas constant (8.314 J/(mol·K)), and T (K) is the absolute temperature.

The rate laws that govern the copper adsorption by the AC were assessed. Three possible adsorption mechanisms were evaluated: the diffusion of Cu species from the aqueous solution to the AC surface (Eq. 9) (Chiarizia *et al.* 1994), the diffusion of ions within the AC (Eq. 10) (Saha *et al.* 2000), and the moving boundary process (Eq. 11) (Chanda and Rempel 1994),

$$\ln(1 - F) = -k \cdot t \quad (9)$$

$$\ln(1 - F^2) = -k \cdot t \quad (10)$$

$$3 - 3 \cdot (1 - F)^{\frac{2}{3}} - 2 \cdot F = k \cdot t \quad (11)$$

where k (min^{-1}) is the corresponding constant, and F (adimensional) is defined according to Eq. 12:

$$F = \frac{[\text{AM}]_t}{[\text{AM}]_e} \quad (12)$$

where $[\text{AM}]_t$ and $[\text{AM}]_e$ (mg/L) are the concentrations of metal adsorbed at time t and at equilibrium, respectively.

Characterization

Zeta potential measurements were performed using a Zetasizer Nano ZS (Malvern Panalytical Ltd., Malvern, UK) at 298 K. Aqueous suspensions were prepared in the pH range of 1 to 5 using HCl (0.1 M). All solutions were dispersed with a sonicator (Sonopuls HD 3100, Bandelin Electronic GmbH & Co. KG, Berlin, Germany) with an amplitude of 80% for 300 s.

The porous structure of the AC was characterized by N_2 adsorption at 77 K using an ASAP 2020 Accelerated Surface Area and Porosimetry System (Micromeritics Instrument Corporation, Norcross, GA, USA). The sample was partially degassed at 623 K for 16 h. The specific surface area was determined by analyzing the adsorption isotherm *via* the Brunauer-Emmett-Teller (BET) equation and density functional theory (DFT), employing Micromeritics and Quantachrome software, Version 1.01, Quantachrome Instruments, Boynton Beach, FL, USA. The results showed that the microporous surface area (S_{mi}) of the AC was 1111 m^2/g , and the BET surface area (S_{BET})

was 2662 m²/g. Moreover, the pores sizes were less than 2 nm (average micropore size $L_0 = 1.71$ nm). Thus, the AC exhibited a microporous structure, indicating its suitability for metal adsorption.

The surfaces of the AC and the AC loaded with Cu (AC-Cu) were examined by field emission scanning electron microscopy (FE-SEM) using a JEOL JSM-7600 (JEOL, Tokyo, Japan) and by X-ray photoelectron spectroscopy (XPS). Spectra were recorded using a Fisons MT500 spectrometer (Fison Instrument, East Grinstead, UK) equipped with a hemispherical electron analyzer (CLAM2) and a non-monochromatic Mg K α X-ray source operated at 300 W. Spectra were collected at a pass energy of 20 eV (typical for high-resolution conditions). The area under each peak was calculated after subtraction of the S-shaped background and fitting the experimental curve to a combination of Lorentzian and Gaussian lines of variable proportions. Binding energies were calibrated to the C 1s peak at 285.0 eV. The atomic ratios were computed from the peak intensity ratios and reported atomic sensitivity factors.

The structural characterization was performed *via* X-ray diffraction (XRD) using a Siemens D5000 diffractometer (Siemens, Munich, Germany) equipped with a Cu anode (Cu K α radiation) and a LiF monochromator.

RESULTS AND DISCUSSION

Adsorption Experiments

Influence of the pH of the solution

The pH greatly affects the adsorption process (Burakov *et al.* 2018). To evaluate the surface charge of the AC, the zeta potential measurements were assessed. The pH value at the point of zero charge (PZC) for the obtained AC was 3.4. The AC surface was positively charged from a pH of 0 to the PZC pH. For pH values greater than 3.4, the AC surface exhibited a negative charge.

The effect of the pH on the Cu adsorption was studied by adding 25 mg of the AC to 100 mL of a solution containing 0.01 g/L of copper ions. The pH values of the solutions were adjusted to 1, 3, and 5 using 0.1 M HCl. Figure 1 shows the amount of copper adsorbed onto the AC *versus* the contact time.

The adsorption capacity increased with the solution pH. The Cu²⁺ removal was quite low at pH values of 1 and 3. This result could be because, at these pH values, the surface of the AC was positively charged, so there was electrostatic repulsion between the surface and the metal charge. When the pH increased beyond the PZC pH (*i.e.*, to pH 5), the negative charge on the AC surface increased, enhancing the metal adsorption (Rao *et al.* 2006). Therefore, the subsequent experiments were performed at this pH value, where the observed adsorption was maximized.

Effect of Cu²⁺ concentration

The adsorptions of different copper concentrations (0.005 g/L to 0.02 g/L) with 25 mg of the AC at a pH of 5 were analyzed (Fig. 2). The obtained q_e values were 13 mg Cu / g AC, 18 mg Cu / g AC, and 26 mg Cu / g AC for 0.005 g/L, 0.01 g/L, and 0.02 g/L, respectively. As expected, the removed Cu²⁺ percentage decreased with increasing initial concentration (65%, 45%, and 33% for 0.005 g/L, 0.01 g/L, and 0.02 g/L, respectively). However, even at the greatest concentration studied, the copper adsorption was nearly 26

mg Cu / g AC, probably due to the fact of the rapid saturation of the activated sites with a certain metal concentration (Al-Homaidan *et al.* 2014).

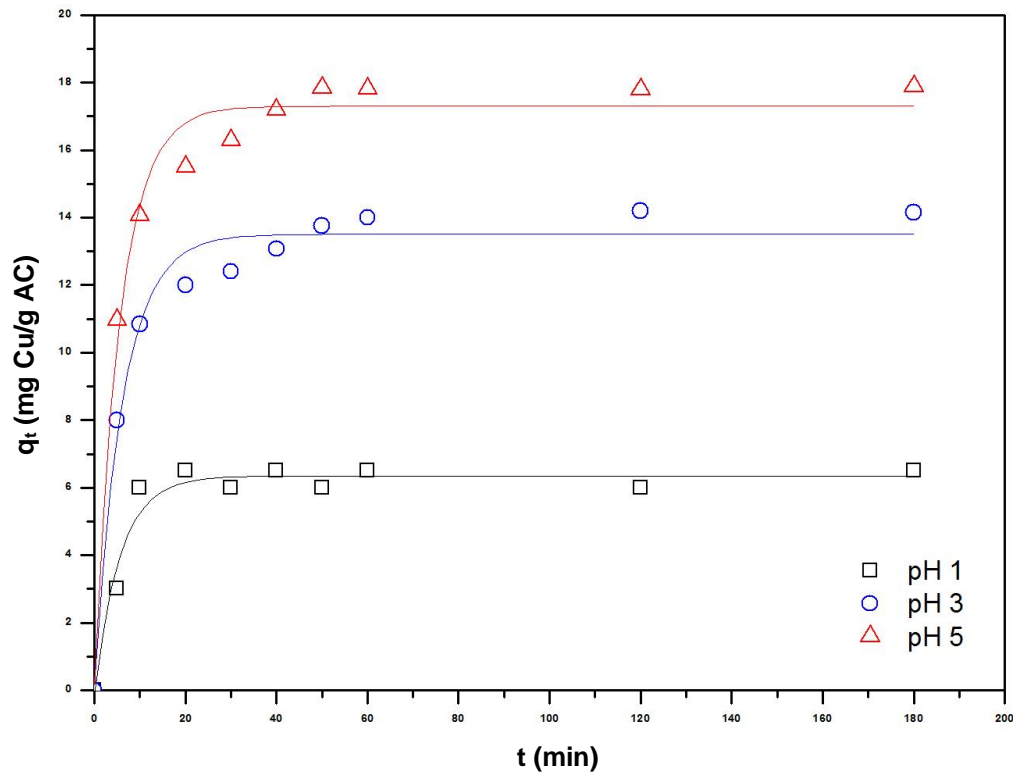


Fig. 1. Copper uptake onto the AC at different pH values as functions of the contact time

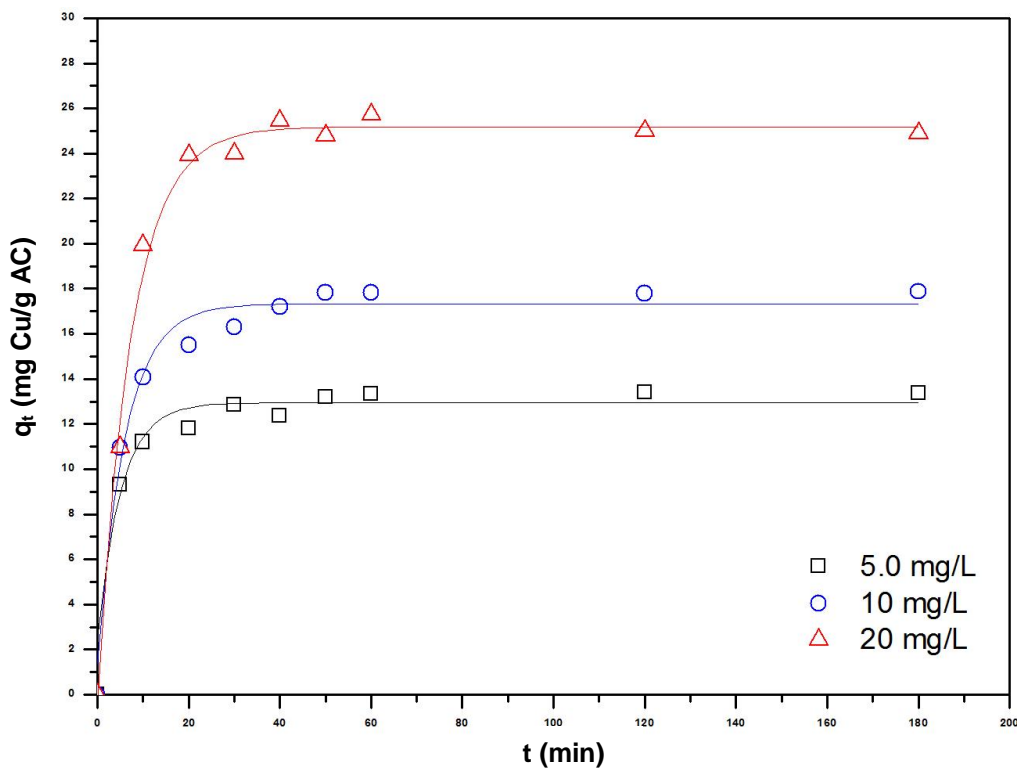


Fig. 2. Effect of copper concentration as functions of the contact time

Effect of activated carbon dosage

To evaluate the effect of the adsorbent dosage on the Cu^{2+} adsorption, solutions 0.01 g/L of Cu^{2+} were put into contact with different masses (12.5 mg to 75 mg) of the AC at a pH of 5. The experimental q_e values were 33 mg Cu / g AC, 29 mg Cu / g AC, 27 mg Cu / g AC, 20 mg Cu / g AC, 19 mg Cu / g AC, and 13 mg Cu / g AC for 12.5 mg, 25 mg, 31 mg, 37.5 mg, 50 mg, and 75 mg of the AC, respectively (Fig. 3). As adsorption percentages, the copper amounts removed were 41%, 73%, 84%, and 75% for 12.5 mg, 25 mg, 31 mg, and 37.5 mg of the adsorbent, respectively, and practically 100% for 50 mg and 75 mg. Thus, the Cu amount adsorbed onto the AC increased with increasing adsorbent dosage. Moreover, when the adsorbent dosage was greater than 50 mg, the copper adsorption was essentially total.

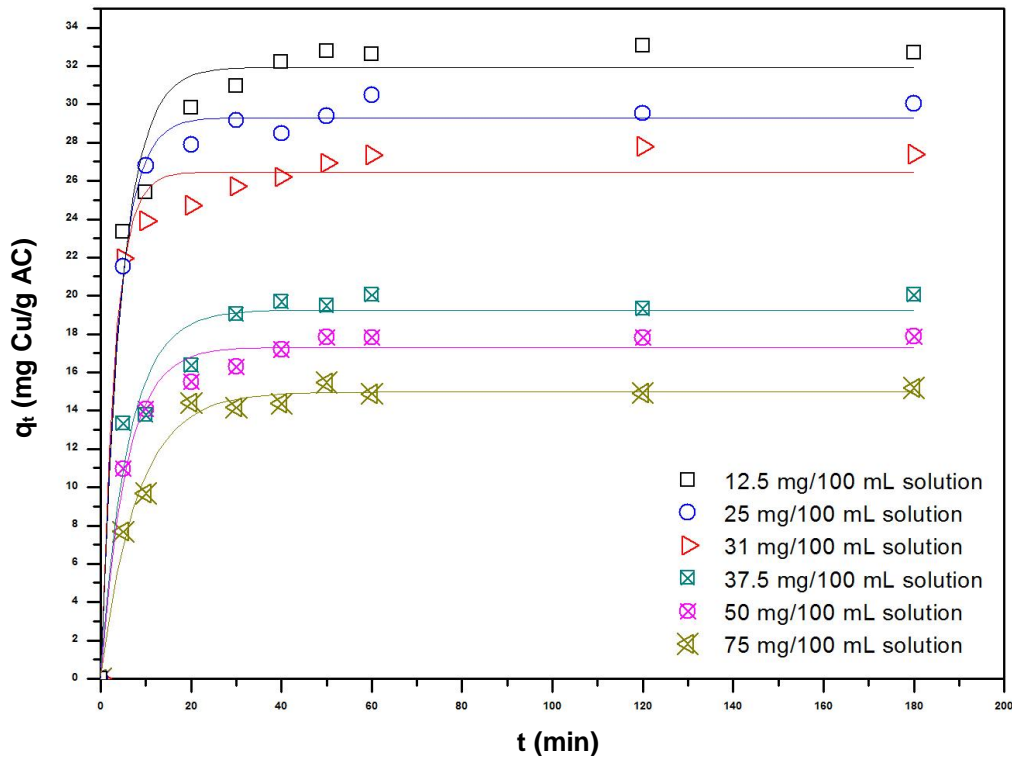


Fig. 3. Effect of the adsorbent dosage on metal uptake

Effect of the temperature

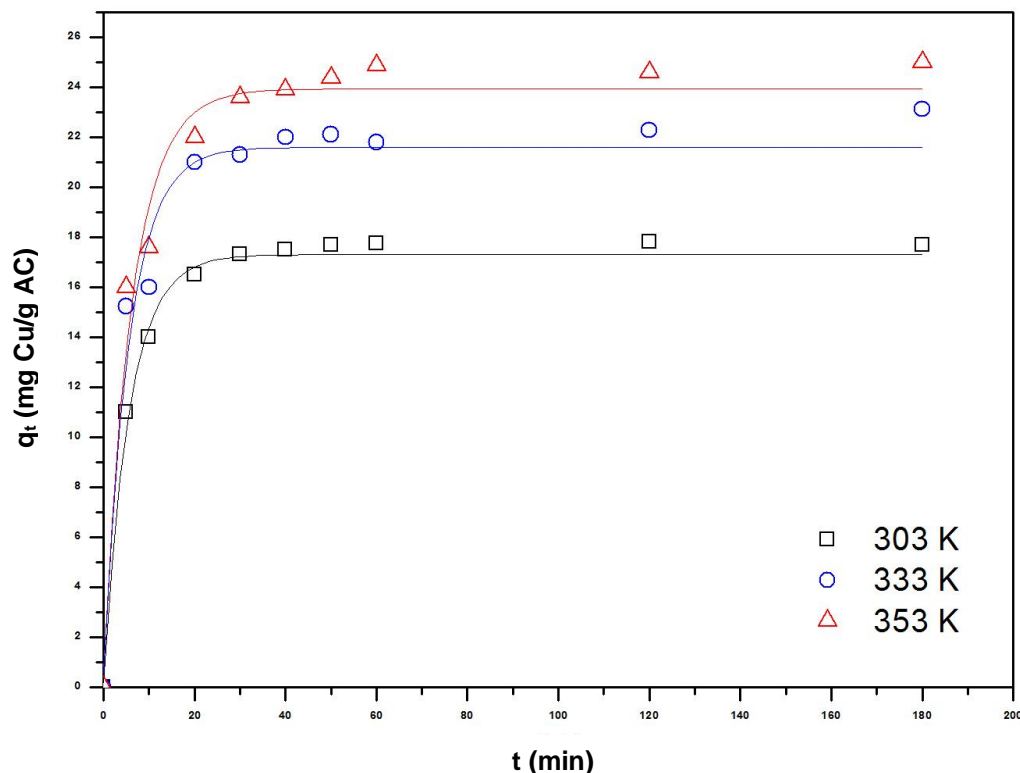
The copper adsorption was analyzed at different temperatures. Solutions with 0.01 g/L of Cu^{2+} were put into contact with 25 mg of the AC at a pH of 5. Figure 4 shows the copper uptakes as functions of time for the different temperatures studied. The amount of copper adsorbed increased when the temperature increased.

Equilibrium isotherms

The equilibrium isotherms were studied using the Langmuir, Freundlich, and Temkin equations. The calculated constant parameters and correlation coefficients are listed in Table 1.

Table 1. Calculated Parameter Values for the Different Lineal Equation Models

Langmuir				Freundlich			Temkin		
q_m (mg/g)	b (L/mg)	R_L	R^2	K_F (L/g)	$1/n$	R^2	A_T (L/g)	b_T	R^2
16.95	3.94	0.03	0.998	5.91	0.92	0.967	0.82	104.92	0.981

**Fig. 4.** Copper uptake at different temperatures

The greatest correlation coefficient was obtained for the Langmuir isotherm. The maximum adsorption capacity (q_m) calculated from this model was similar to the experimental one (18 mg/g). Additionally, the dimensionless Langmuir separation factor (R_L) of 0.03 indicated a favorable adsorption process (Deihimi *et al.* 2018; Sudha Rani *et al.* 2018). Table 2 exhibits a comparative of the maximum adsorption capacities of different bioadsorbents for copper adsorption. It is noted that capacity of the obtained activated carbon from winemaking wastes was higher than others bioadsorbents previously used.

Table 2. Maximum Adsorption Capacity (q_m) of Different Adsorbents for Cu(II) Adsorption

Biowaste	q_m (mg/g)	References
Barks of woods	4.4 to 7.6	(Seki et al. 1997)
Moss	8.45	(Al-Asheh and Duvnjak 1998)
Pine bark	9.65	(Al-Asheh and Duvnjak 1998)
Mango tree sawdust	5.3	(Ajmal et al. 1998)
Sphagnum peat moss	12.6	(Ho and McKay 2004)

Kinetic study

The results derived from Fig. 4 were used to fit various kinetic models, and the calculated results from these fits are summarized in Table 3. In all cases, the pseudo-second-order model exhibited markedly greater correlation coefficients than those of the pseudo-first-order model. The calculated q_e values ($q_{e,calc}$) were in good agreement with the obtained experimental q_e values ($q_{e,exp}$). Additionally, K_2 decreased with increasing temperature, which indicated that the metal adsorption occurred more easily at greater temperatures. This excellent fit to the pseudo-second-order equation has been shown recently to be an indication that the rate is likely controlled by diffusion (Hubbe *et al.* 2019).

Table 3. Kinetic Parameters for Copper Adsorption at Different Temperatures

Pseudo-first-order				Pseudo-second-order			
T (K)	R^2	K_1 (min^{-1})	q_e (mg/g)	R^2	K_2 ($\text{g}/(\text{mg}\cdot\text{min})$)	$q_{e,calc}$ (mg/g)	$q_{e,exp}$ (mg/g)
303	0.687	0.04	9.20	0.994	0.131	16.52	17.30
333	0.567	0.07	10.34	0.997	0.048	22.72	22.62
353	0.702	0.05	10.57	0.999	0.020	23.61	24.53

To estimate the adsorption type, the kinetic rate constants ($\ln k_{2,obs}$) were fitted *versus* $1/T$, with slope $-E_a/R$ (Boparai *et al.* 2011): The activation energy (E_a) is frequently used for differentiating between physical and chemical adsorption. With physical adsorption, the reactions are readily reversible, and equilibrium is attained rapidly, so the energy requirements are small (in the range of 5 kJ/mol to 40 kJ/mol). However, chemical adsorption is specific and involves stronger forces, and it thus requires greater activation energies (40 kJ/mol to 800 kJ/mol) (Boparai *et al.* 2011). In this case, the calculated activation energy was -32 kJ/mol. In general, activation energy is positive. However, in some cases, the activation energy can be negative when K_2 values decreases with increasing temperature (Revell and Williamson 2013). The obtained result suggested a physisorption process.

Table 4 summarizes the thermodynamic parameters. The calculated values for the enthalpy change (-13.9 kJ/mol) and free energy change (-30.46 kJ/mol, -32.10 kJ/mol, and -33.19 kJ/mol) indicated that the copper adsorption by the AC was an exothermic, spontaneous, and favorable process.

Table 4. Thermodynamic Parameters at Different Temperatures

T (K)	$-\Delta H^\circ$ (kJ/mol)	ΔS° ($\text{J}/(\text{mol}\cdot\text{K})$)	$-\Delta G^\circ$ (kJ/mol)
303	13.93	54.55	30.46
333			32.10
353			33.19

Characterization of the AC and AC-Cu

Scanning electron microscopy (SEM)

Scanning electron micrographs of the initial AC and AC-Cu are shown in Fig. 5. A clear change could be seen when the copper was adsorbed on the AC surface. Initially, a porous structure was observed, characteristic of an AC. After the Cu adsorption, the pore structure changed, different contrast was appreciated. Additionally, microanalysis indicated the presence of a peak at 1 keV, characteristics of Cu K_{α} in the sample.

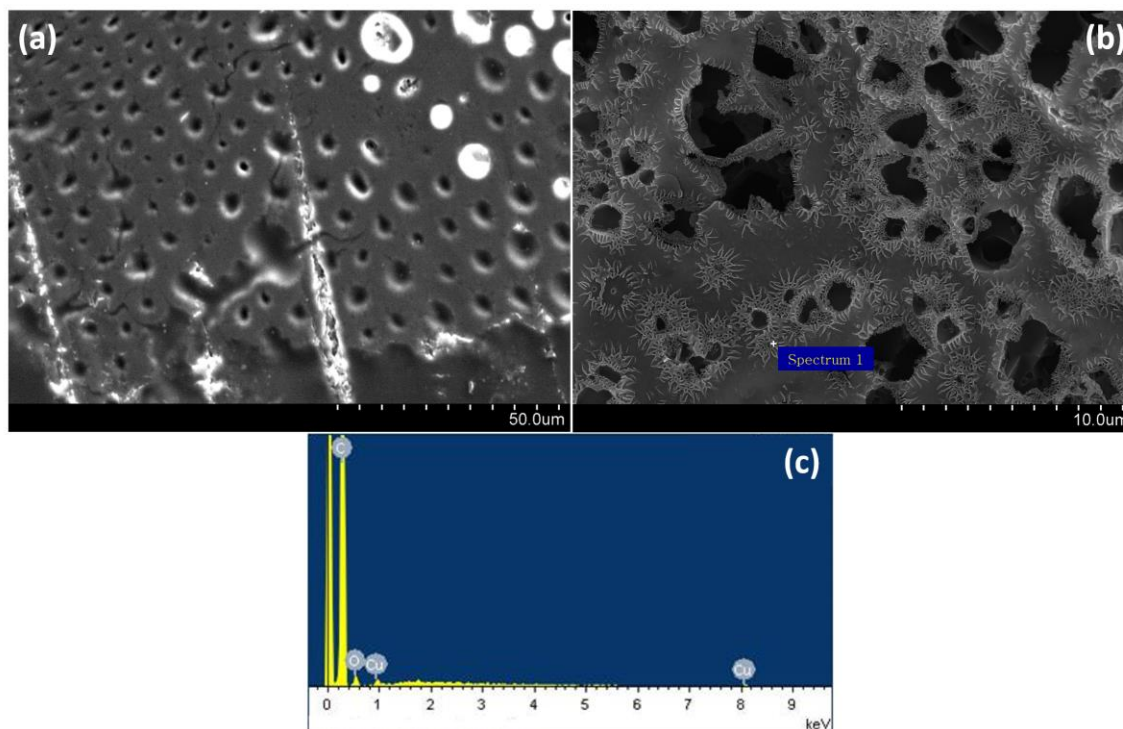


Fig. 5. SEM micrographs of the (a) AC and (b) AC-Cu. (c) EDS microanalysis of the AC-Cu sample

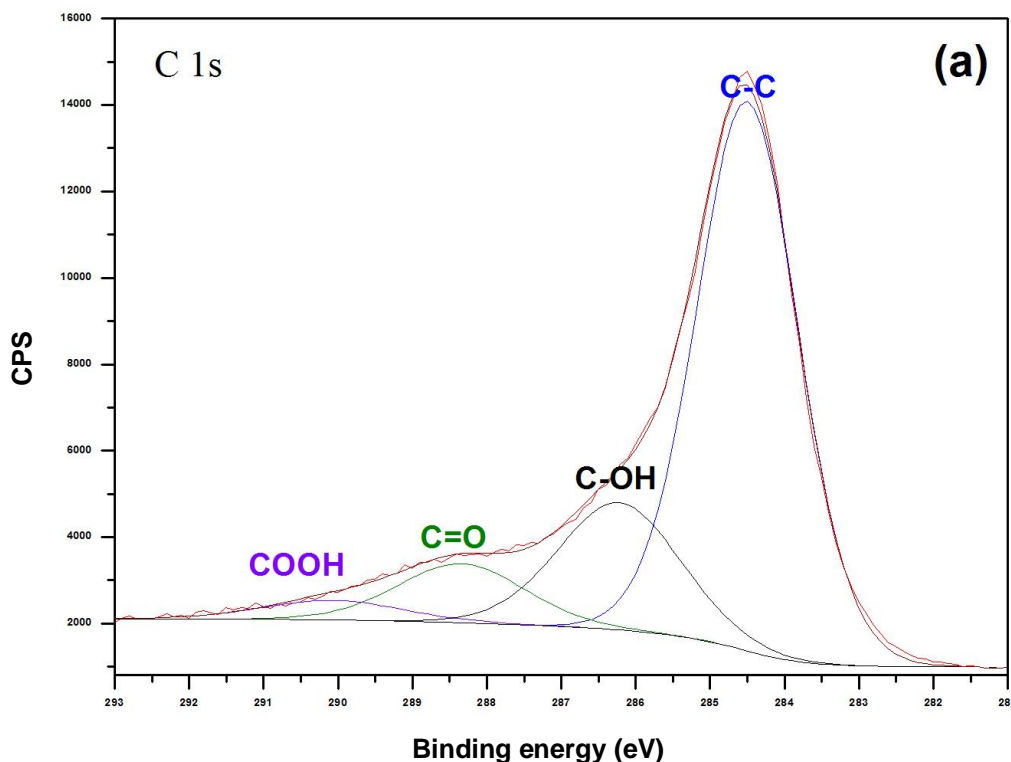
XPS analysis

The XPS spectra of the C 1s regions for both the AC and AC-Cu samples are shown in Fig. 6(a) and 6(b). The spectra were similar in terms of the shape and position of the bands. A broad and asymmetric band was observed in both cases, suggesting the presence of different carbon species. The deconvolution of the bands exhibited four peaks, at approximately 285 eV (C-C bond), 286 eV (C-OH bond), 288 eV (C=O bond), and 290 eV (COOH bond) (Ko *et al.* 2012; Farzana *et al.* 2018; Oh *et al.* 2019).

Meanwhile, the XPS spectrum of Cu 2p core level excitation in the AC-Cu sample is shown in Fig. 6(c), to understand the electronic structure of the copper species on the surface. The obtained spectrum showed two main peaks, centered at approximately 933 eV and 953 eV, which could be attributed to Cu 2p^{3/2} and 2p^{1/2}, respectively. Additionally, the Cu 2p^{3/2} peak exhibited a shoulder band, which could indicate that the Cu²⁺ components were different in chemical environment, as a previously reported (Li *et al.* 2015; Choong *et al.* 2018). These observed peaks appeared at approximately 934.3 eV and 932.6 eV and could be assigned to octa-coordination of Cu²⁺ ions and tetra-coordination of Cu⁺-Cu⁰ species (Li *et al.* 2015; Choong *et al.* 2018). Notably, it is

difficult to distinguish between Cu^+ and Cu^0 peaks, because the Cu 2p binding energies of both species are very close (Liu *et al.* 2019).

Although the kinetic studies indicated a physisorption process, the results of the XPS analyses could suggest a chemisorption process. Lastly, the band at 945 eV could be assigned to satellite bands. This band was generated by an electron transfer from a ligand orbital to a 3d orbital of Cu. Therefore, because Cu^0 and Cu^+ species have a completely filled d level, the observed satellite band confirmed that Cu^{2+} was present on the surface of the material (Espinós *et al.* 2002; Chanquía *et al.* 2010; Li *et al.* 2015).



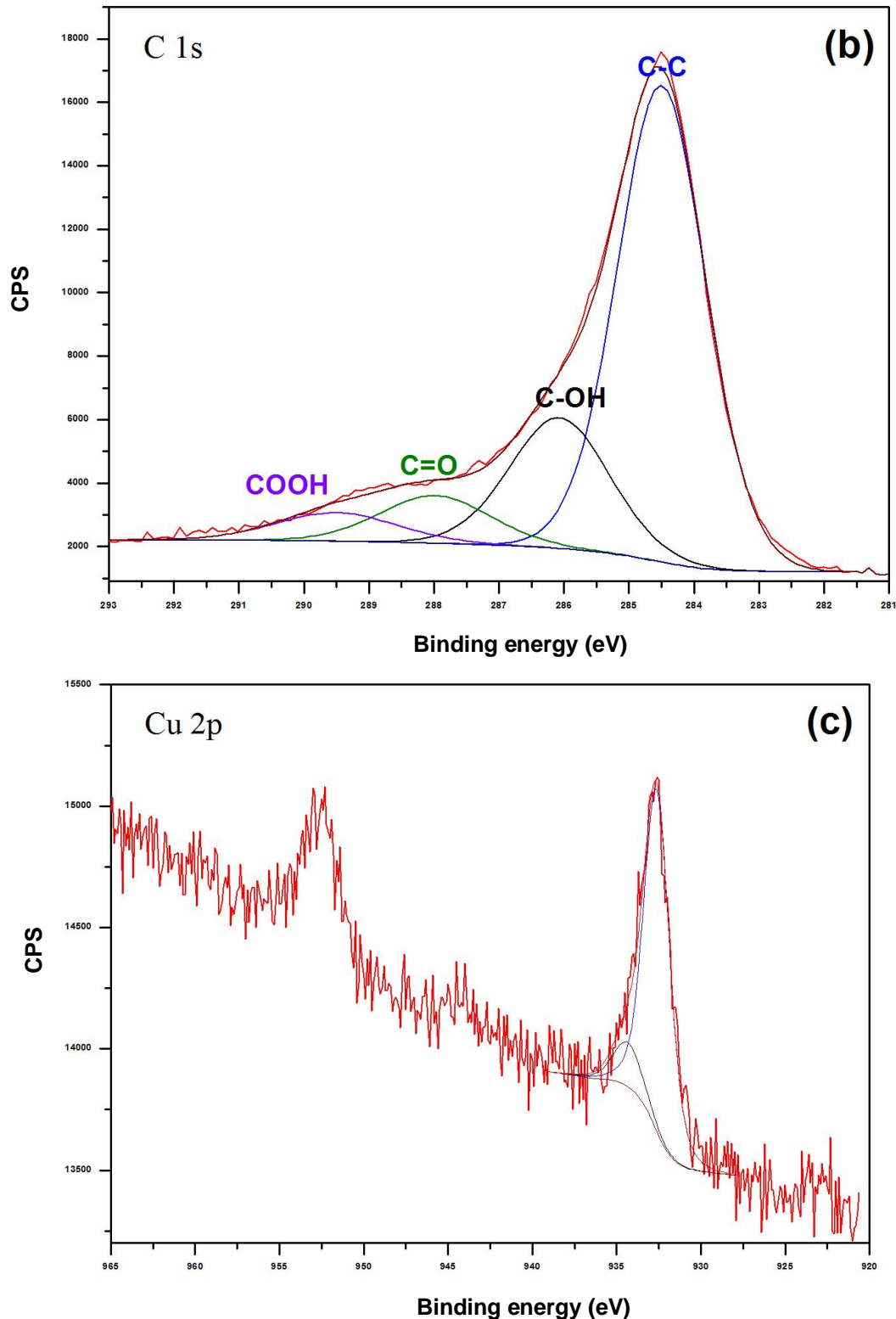


Fig. 6. XPS spectra of the AC and AC-Cu

Post-treatment of the Adsorption Process

SEM

The possibility of recovering copper from the Cu(II)-bearing solutions were investigated Cu(II) was eluted with a 0.1 M H₂SO₄ solution, then these were precipitated

with sodium borohydride. As a result of this precipitation, a nearly black solid was yielded, which apparently was formed by cuprite and zero-valent copper. This step must be investigated in depth.

The overall reaction responsible for the precipitation could be written as follows (Eq. 13):



The subsequent SEM study indicated that the solid was formed by nanoparticle agglomerates with different shapes, nanoplates, and octahedral shapes, characteristics of the $\text{Cu}_2\text{O}/\text{Cu}$ phases' nanostructures (Won and Stanciu 2012; Wei *et al.* 2016).

Adsorption mechanisms

The adsorption process can be controlled by several diffusion mechanisms. These include film diffusion (bulk diffusion and external film diffusion), particle diffusion (intraparticle or internal diffusion), and a moving boundary process, a part of chemical reaction that could contribute to the control of mass transfer (Krys *et al.* 2013).

The calculated parameters for each model (Qiu *et al.* 2009) are shown in Table 5. The obtained correlation coefficients showed that the copper adsorption could be best explained by the moving boundary process.

Table 5. Kinetic Constants of the Different Adsorption Mechanisms

Model	R ²	k
Film diffusion	0.946	0.058
Particle diffusion	0.951	0.050
Moving boundary	0.982	0.012

Statistical analysis

To determine the influences of copper concentration (A), pH (B), and carbon dosage (C) on the adsorption of Cu(II) onto the AC, a full factorial design of 2^3 , with 2 central points was performed (Maneechakr *et al.* 2015; Ghaedi *et al.* 2018). The independent variables were varied at two levels where upper (+1) and lower (-1) limits for each one. With the statistical analysis of the considered factors, the Pareto chart identifies factors and interaction effects that are statically significant ($p < 0.05$) (Adio *et al.* 2017; Saleh *et al.* 2018). The only statically significant factor was the pH (Fig. 7). The positive sign indicates a positive effect between an increase in the pH and the percentage of copper adsorbed.

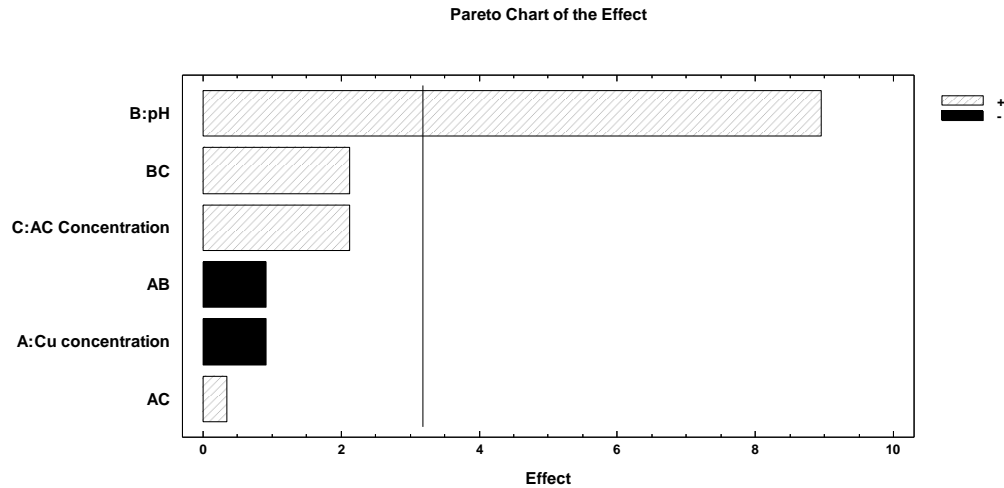


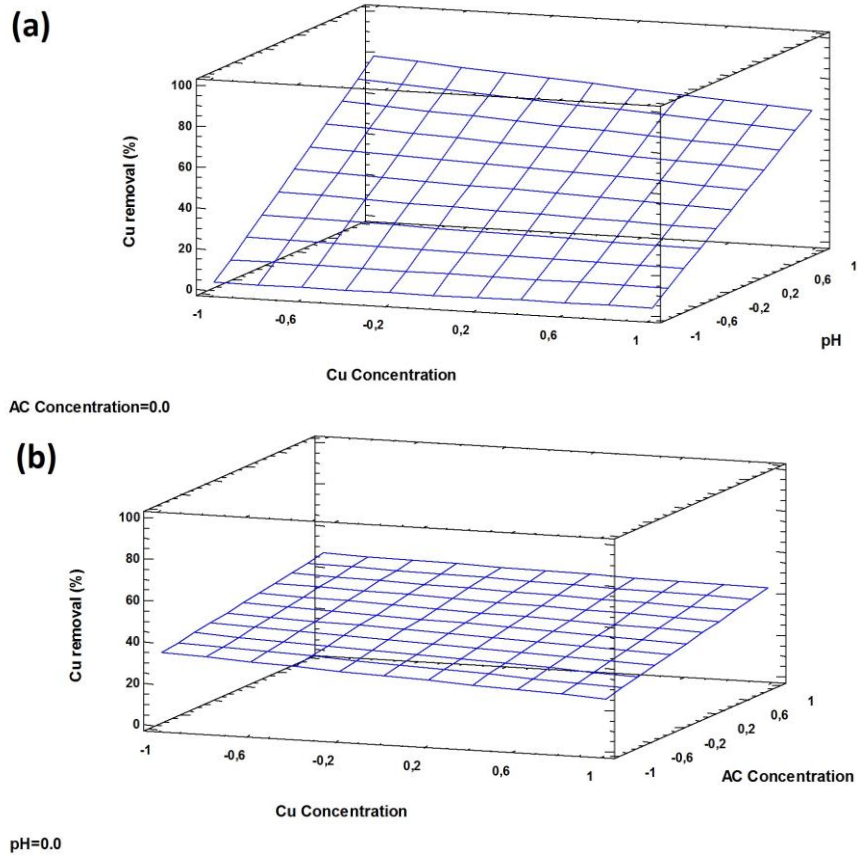
Fig. 7. Pareto chart diagram for copper adsorption

The mathematical model obtained for this design was as follows (Eq. 14):

$$\begin{aligned}
 \text{Elimination (\%)} = & 37.52 - 3.553 \cdot [\text{Cu(II)}] + 34.595 \cdot \text{pH} + 8.183 \cdot [\text{AC}] - 3.553 \cdot [\text{Cu(II)}] \cdot \text{pH} \\
 & + 1.33 \cdot [\text{Cu(II)}] \cdot [\text{AC}] + 8.183 \cdot \text{pH} \cdot [\text{AC}] \quad (14)
 \end{aligned}$$

with $R^2 = 96.81$.

Figure 8 shows response surfaces as functions of two factors, keeping the third factor constant.



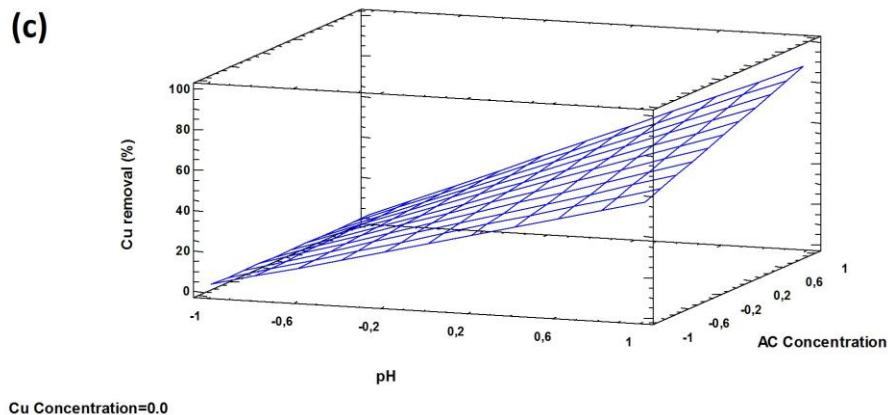


Fig. 8. Response surface plots for copper metal removal (%): (a) effects of Cu concentration and pH, (b) effects of Cu concentration and AC concentration, and (c) effects of pH and AC concentration

This is the best way to evaluate the relationship between a factor and the response (Mourabet *et al.* 2012). Figure 8(a) shows increases in Cu^{2+} adsorption with increasing pH, with the increase appearing slightly greater at the lowest copper concentration. For pH and AC concentration (Fig. 8(c)), the behavior was similar: An increase in the pH increased the copper removal percentage, and the effect was greater at greater AC concentrations.

Figure 9 shows the cube graph of the copper removal percentage. The optimum recovery percentage of Cu(II) obtained with the model was 94.26%, corresponding to a Cu concentration of 5 mg/L, a pH of 5, and an AC dosage of 75 mg.

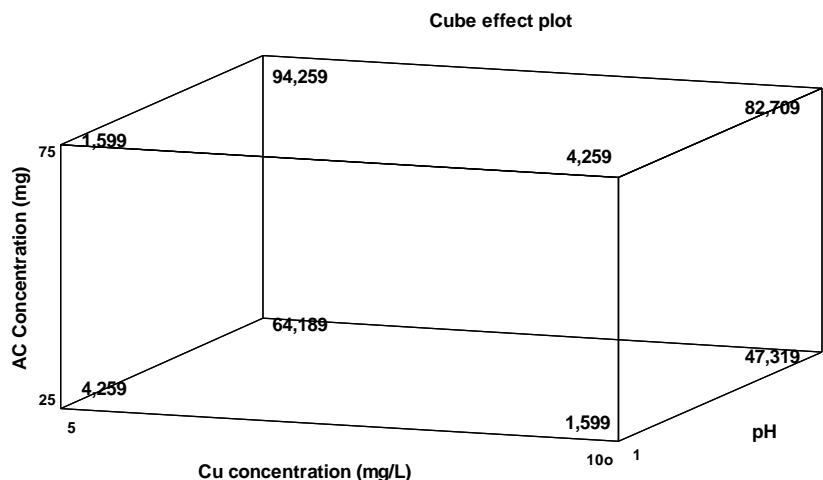


Fig. 9. The cube graph of copper removal percentage

CONCLUSIONS

1. Activated carbon from winemaking wastes was satisfactorily used to remove copper from aqueous solutions.

2. Optimum pH value of 5 was found, reaching a copper adsorption of 18 mg Cu/g AC for the studied conditions.
3. When the initial copper concentration doubles, the removed amount is similar.
4. Kinetic studies showed that the Cu adsorption was better described by the pseudo-second-order kinetic model. The experimental results fit a Langmuir isotherm. Thermodynamic studies showed that the copper adsorption was an exothermic, spontaneous, and favorable process.
5. XPS results show the possible presence of different copper species (Cu^0 - Cu^+ and Cu^{2+}) on the surface of the material.
6. It was possible to recover zero-valent copper from the elution with a H_2SO_4 solution and precipitated with sodium borohydride.
7. The full factorial experimental design showed that the pH and the pH-AC-dosage interaction greatly affected the Cu removal process. The optimal conditions were determined as follows: Cu concentration of 5 mg/L, pH of 5, and 10 mg of AC.

ACKNOWLEDGMENTS

The authors would like to thank Dr. Irene Llorente of the National Center for Metallurgical Research, Spanish National Research Council (CENIM-CSIC), for performing the XPS measurements.

REFERENCES CITED

- Adio, S. O., Omar, M. H., Asif, M., and Saleh, T. A. (2017). "Arsenic and selenium removal from water using biosynthesized nanoscale zero-valent iron: A factorial design analysis," *Process Safety and Environmental Protection* 107, 518-527. DOI: 10.1016/j.psep.2017.03.004
- Al-Homaidan, A. A., Al-Houri, H. J., Al-Hazzani, A. A., Elgaaly, G., and Moubayed, N. M. S. (2014). "Biosorption of copper ions from aqueous solutions by *Spirulina platensis* biomass," *Arabian Journal of Chemistry* 7(1), 57-62. DOI: 10.1016/j.arabjc.2013.05.022
- Alcaraz, L., López Fernández, A., García-Díaz, I., and López, F. A. (2018). "Preparation and characterization of activated carbons from winemaking wastes and their adsorption of methylene blue," *Adsorption Science & Technology* 36(5-6), 1331-1351. DOI: 10.1177/0263617418770295
- Alcaraz, L., Alguacil, F.J., Llorente, I., Urbieto, A., Fernandez, P., and López F. A., (2019). "Dysprosium removal from water using active carbons obtained from spent coffee ground." *Nanomaterials* 9, 1372. DOI: 10.3390/nano9101372
- Alguacil, F. J., Alcaraz, L., García-Díaz, I., and López, F. A. (2018). "Removal of Pb^{2+} in wastewater via adsorption onto an activated carbon produced from winemaking waste," *Metals* 8(9). DOI: 10.3390/met8090697
- Al-Asheh, S., and Duvnjak, Z. (1998). "Binary metal sorption by pine bark: study of equilibria and mechanisms," *Separation Science and Technology* 33(9), 1303-1329. DOI: 10.1080/01496399808544985
- Aljeboree, A. M., Alshirifi, A. N., and Alkaim, A. F. (2017). "Kinetics and equilibrium study for the adsorption of textile dyes on coconut shell activated carbon," *Arabian*

- Journal of Chemistry* 10, S3381-S3393. DOI: 10.1016/j.arabjc.2014.01.020
- Ajmal, M., Hussain Khan, A., Ahmad, S., and Ahmad, A. (1998). "Role of sawdust in the removal of copper(II) from industrial wastes," *Water Research* 32(10), 3085-3091. DOI: 10.1016/S0043-1354(98)00067-0
- Aydın, H., Bulut, Y., and Yerlikaya, Ç. (2008). "Removal of copper (II) from aqueous solution by adsorption onto low-cost adsorbents," *Journal of Environmental Management* 87(1), 37-45. DOI: 10.1016/j.jenvman.2007.01.005
- Boparai, H. K., Joseph, M., and O'Carroll, D. M. (2011). "Kinetics and thermodynamics of cadmium ion removal by adsorption onto nano zerovalent iron particles," *Journal of Hazardous Materials* 186(1), 458-465. DOI: 10.1016/j.jhazmat.2010.11.029
- Burakov, A. E., Galunin, E. V., Burakova, I. V., Kucherova, A. E., Agarwal, S., Tkachev, A. G., and Gupta, V. K. (2018). "Adsorption of heavy metals on conventional and nanostructured materials for wastewater treatment purposes: A review," *Ecotoxicology and Environmental Safety* 148, 702-712. DOI: 10.1016/j.ecoenv.2017.11.034
- Caprarescu, S., Corobea, M. C., Purcar, V., Spataru, C. I., Ianchis, R., Vasilevici, G., and Vuluga, Z. (2015). "San copolymer membranes with ion exchangers for Cu(II) removal from synthetic wastewater by electrodialysis," *Journal of Environmental Sciences*, 35(Ii), 27-37. DOI: 10.1016/j.jes.2015.02.005
- Caprarescu, S., Radu, A. L., Purcar, V., Sarbu, A., Vaireanu, D. I., Ianchis, R., and Ghiurea, M. (2014). "Removal of copper ions from simulated wastewaters using different bicomponent polymer membranes," *Water, Air, and Soil Pollution* 225(8). DOI: 10.1007/s11270-014-2079-6
- Caprarescu, S., Vaireanu, D. I., Cojocar, A., Maior, I., and Sarbu, A. (2009). "Removal of copper ions from electroplating wastewater by ion-exchange membranes," *Revista de Chimie*, 60(7), 673-677
- Carvalho Barros, G. K. G., Melo, R. P. F., and de Barros Neto, E. L. (2018). "Removal of copper ions using sodium hexadecanoate by ionic flocculation," *Separation and Purification Technology* 200, 294-299. DOI: 10.1016/j.seppur.2018.01.062
- Chanda, M., and Rempel, G. L. (1994). "Quaternized poly(4-vinylpyridine) gel-coated on silica. Fast kinetics of diffusion-controlled sorption of organic sulfonates," *Industrial & Engineering Chemistry Research* 33(3), 623-630. DOI: 10.1021/ie00027a020
- Chanquía, C. M., Sapag, K., Rodríguez-Castellón, E., Herrero, E. R., and Eimer, G. A. (2010). "Nature and location of copper nanospecies in mesoporous molecular sieves," *The Journal of Physical Chemistry C* 114(3), 1481-1490. DOI: 10.1021/jp9094529
- Chiarizia, R., Horwitz, E. P., and Alexandratos, S. D. (1994). "Uptake of metal ions by a new chelating ion-exchange resin. Part 4: Kinetics," *Solvent Extraction and Ion Exchange* 12(1), 211-237. DOI: 10.1080/07366299408918209
- Choong, C. E., Lee, G., Jang, M., Park, C. M., and Ibrahim, S. (2018). "One step hydrothermal synthesis of magnesium silicate impregnated palm shell waste activated carbon for copper ion removal," *Metals* 8(10). DOI: 10.3390/met8100741
- Coudert, L., Blais, J.-F., Mercier, G., Cooper, P., Gastonguay, L., Morris, P., Janin, A., and Reynier, N. (2013). "Pilot-scale investigation of the robustness and efficiency of a copper-based treated wood wastes recycling process," *Journal of Hazardous Materials* 261, 277-285. DOI: 10.1016/j.jhazmat.2013.07.035
- Deihimi, N., Irannajad, M., and Rezai, B. (2018). "Equilibrium and kinetic studies of ferricyanide adsorption from aqueous solution by activated red mud," *Journal of Environmental Management* 227, 277-285. DOI: 10.1016/j.jenvman.2018.08.089

- Demiral, H., and Güngör, C. (2016). "Adsorption of copper(II) from aqueous solutions on activated carbon prepared from grape bagasse," *Journal of Cleaner Production* 124, 103-113. DOI: 10.1016/j.jclepro.2016.02.084
- Espinós, J. P., Morales, J., Barranco, A., Caballero, A., Holgado, J. P., and González-Elipe, A. R. (2002). "Interface effects for Cu, CuO, and Cu₂O deposited on SiO₂ and ZrO₂. XPS determination of the valence state of copper in Cu/SiO₂ and Cu/ZrO₂ catalysts," *The Journal of Physical Chemistry B* 106(27), 6921-6929. DOI: 10.1021/jp014618m
- Farzana, R., Rajarao, R., Bhat, B. R., and Sahajwalla, V. (2018). "Performance of an activated carbon supercapacitor electrode synthesised from waste compact discs (CDs)," *Journal of Industrial and Engineering Chemistry* 65, 387-396. DOI: 10.1016/j.jiec.2018.05.011
- Feng, N., Guo, X., and Liang, S. (2009). "Adsorption study of copper (II) by chemically modified orange peel," *Journal of Hazardous Materials* 164(2-3), 1286-1292. DOI: 10.1016/j.jhazmat.2008.09.096
- Ferreira da Silva, A. J., Paiva de Alencar Moura, M. C., da Silva Santos, E., Saraiva Pereira, J. E., and de Barros Neto, E. L. (2018). "Copper removal using carnauba straw powder: Equilibrium, kinetics, and thermodynamic studies," *Journal of Environmental Chemical Engineering* 6(6), 6828-6835. DOI: 10.1016/j.jece.2018.10.028
- Fouodjouo, M., Fotouo-Nkaffo, H., Laminsi, S., Cassini, F. A., de Brito-Benetoli, L. O., and Debacher, N. A. (2017). "Adsorption of copper (II) onto cameroonian clay modified by non-thermal plasma: Characterization, chemical equilibrium and thermodynamic studies," *Applied Clay Science* 142, 136-144. DOI: 10.1016/j.clay.2016.09.028
- Ghaedi, A. M., Panahimehr, M., Nejad, A. R. S., Hosseini, S. J., Vafaei, A., and Baneshi, M. M. (2018). "Factorial experimental design for the optimization of highly selective adsorption removal of lead and copper ions using metal organic framework MOF-2 (Cd)," *Journal of Molecular Liquids* 272, 15-26. DOI: 10.1016/j.molliq.2018.09.051
- He, H. J., Xiang, Z. H., Chen, X. J., Chen, H., Huang, H., Wen, M., and Yang, C. P. (2018). "Biosorption of Cd(II) from synthetic wastewater using dry biofilms from biotrickling filters," *International Journal of Environmental Science and Technology*, 15(7), 1491-1500. DOI: 10.1007/s13762-017-1507-8
- Ho, Y. S., and McKay, G. (1999). "Pseudo-second order model for sorption processes," *Process Biochemistry* 34(5), 451-465. DOI: 10.1016/S0032-9592(98)00112-5
- Ho, Y. S., and McKay, G. (2004). "Sorption of copper(II) from aqueous solution by Peat," *Water, Air, and Soil Pollution*, 158(1), 77-97. DOI: 10.1023/B:WATE.0000044830.63767.a3
- Hu, Z., and Srinivasan, M. P. (1999). "Preparation of high-surface-area activated carbons from coconut shell," *Microporous and Mesoporous Materials* 27(1), 11-18. DOI: 10.1016/S1387-1811(98)00183-8
- Hubbe, M. A., Azizian, S., and Douven, S. (2019). "Implications of apparent pseudo-second-order adsorption kinetics onto cellulosic materials. A review," *BioResources* 14(3), 7582-7626.
- Kalaiselvi, G., Maheswari, P., Mohan, D., and Balasubramanian, S. (2015). "Synthesis and characterization of poly 3-methyl 2-vinyl pyridinium nitrate incorporated polyvinylidene fluoride ultrafiltration membrane for metal ion removal," *Separation and Purification Technology* 143, 105-114. DOI: 10.1016/j.seppur.2015.01.034

- Kaouah, F., Boumaza, S., Berrama, T., Trari, M., and Bendjama, Z. (2013). "Preparation and characterization of activated carbon from wild olive cores (*oleaster*) by H₃PO₄ for the removal of Basic Red 46," *Journal of Cleaner Production* 54, 296-306. DOI: 10.1016/j.jclepro.2013.04.038
- Ko, T.-J., Her, E. K., Shin, B., Kim, H.-Y., Lee, K.-R., Hong, B. K., Kim, S. H., Oh, K. H., and Moon, M.-W. (2012). "Water condensation behavior on the surface of a network of superhydrophobic carbon fibers with high-aspect-ratio nanostructures," *Carbon* 50(14), 5085-5092. DOI: 10.1016/j.carbon.2012.06.048
- Krys, P., Testa, F., Trochimczuk, A., Pin, C., Taulemesse, J.-M., Vincent, T., and Guibal, E. (2013). "Encapsulation of ammonium molybdophosphate and zirconium phosphate in alginate matrix for the sorption of rubidium(I)," *Journal of Colloid and Interface Science* 409, 141-150. DOI: 10.1016/j.jcis.2013.07.046
- Lagergren, S. (1898). "Zur Theorie der sogenannten Adsorption gelöster Stoffe," *Bihang till Kungliga Svenska Vetenskaps-akademiens Handlingar* 24(4), 1-39.
- Li, B., Luo, X., Zhu, Y., and Wang, X. (2015). "Immobilization of Cu(II) in KIT-6 supported Co₃O₄ and catalytic performance for epoxidation of styrene," *Applied Surface Science* 359, 609-620. DOI: 10.1016/j.apsusc.2015.10.131
- Li, X., Yang, W. L., He, H., Wu, S., Zhou, Q., Yang, C., Zeng, G., Luo, L., and Lou, W. (2018). "Responses of microalgae *Coelastrella* sp. to stress of cupric ions in treatment of anaerobically digested swine wastewater," *Bioresource Technology* 274-279. DOI: 10.1016/j.biortech.2017.12.058
- Liew, R. K., Chai, C., Yek, P. N. Y., Phang, X. Y., Chong, M. Y., Nam, W. L., Su, M. H., Lam, W. H., Ma, N. L., and Lam, S. S. (2019). "Innovative production of highly porous carbon for industrial effluent remediation via microwave vacuum pyrolysis plus sodium-potassium hydroxide mixture activation," *Journal of Cleaner Production* 208, 1436-1445. DOI: 10.1016/j.jclepro.2018.10.214
- Liu, L., Li, W., Xiong, Z., Xia, D., Yang, C., Wang, W., and Sun, Y. (2019). "Synergistic effect of iron and copper oxides on the formation of persistent chlorinated aromatics in iron ore sintering based on *in situ* XPS analysis," *Journal of Hazardous Materials* 366, 202-209. DOI: 10.1016/j.jhazmat.2018.11.105
- Liu, Y., Xu, J., Cao, Z., Fu, R., Zhou, C., Wang, Z., and Xu, X. (2020). "Adsorption behavior and mechanism of Pb(II) and complex Cu(II) species by biowaste-derived char with amino functionalization," *Journal of Colloid and Interface Science*, 559, 215-225. DOI: 10.1016/j.jcis.2019.10.035
- Maneechakr, P., Samerjit, J., Uppakarnrod, S., and Karnjanakom, S. (2015). "Experimental design and kinetic study of ultrasonic assisted transesterification of waste cooking oil over sulfonated carbon catalyst derived from cyclodextrin," *Journal of Industrial and Engineering Chemistry* 32, 128-136. DOI: 10.1016/j.jiec.2015.08.008
- Modrogan, C., Apostol, D. G., Butucea, O. D., Miron, A. R., Costache, C., and Kouachi, R. (2013). "Kinetic study of hexavalent chromium removal from wastewaters by ion exchange," *Environmental Engineering and Management Journal*, 12(5), 929-935. DOI: 10.30638/eemj.2013.115
- Modrogan, C., Miron, A. R., Orbulet, O. D., Costache, C., and Apostol, G. (2015). "Ion exchange processes on weak acid resins for wastewater containing copper ions treatment," *Environmental Engineering and Management Journal* 14(2), 449-454. DOI: 10.30638/eemj.2015.046
- Mourabet, M., El Rhilassi, A., El Boujaady, H., Bennani-Ziatni, M., El Hamri, R., and

- Taitai, A. (2012). "Removal of fluoride from aqueous solution by adsorption on Apatitic tricalcium phosphate using Box–Behnken design and desirability function," *Applied Surface Science* 258(10), 4402-4410. DOI: 10.1016/j.apsusc.2011.12.125
- Ntimbani, R. N., Simate, G. S., and Ndlovu, S. (2015). "Removal of copper ions from dilute synthetic solution using staple ion exchange fibres: Equilibrium and kinetic studies," *Journal of Environmental Chemical Engineering* 3(2), 1258-1266. DOI: 10.1016/j.jece.2015.02.010
- Oh, J.-Y., You, Y.-W., Park, J., Hong, J.-S., Heo, I., Lee, C.-H., and Suh, J.-K. (2019). "Adsorption characteristics of benzene on resin-based activated carbon under humid conditions," *Journal of Industrial and Engineering Chemistry* 71, 242-249. DOI: 10.1016/j.jiec.2018.11.032
- Pallarés, J., González-Cencerrado, A., and Arauzo, I. (2018). "Production and characterization of activated carbon from barley straw by physical activation with carbon dioxide and steam," *Biomass and Bioenergy* 115, 64-73. DOI: 10.1016/j.biombioe.2018.04.015
- Qiu, H., Lv, L., Pan, B.-c., Zhang, Q.-j., Zhang, W.-m., and Zhang, Q.-x. (2009). "Critical review in adsorption kinetic models," *Journal of Zhejiang University-Science A* 10(5), 716-724. DOI: 10.1631/jzus.a0820524
- Rao, M. M., Ramesh, A., Rao, G. P. C., and Seshaiiah, K. (2006). "Removal of copper and cadmium from the aqueous solutions by activated carbon derived from *Ceiba pentandra* hulls," *Journal of Hazardous Materials* 129(1-3), 123-129. DOI: 10.1016/j.jhazmat.2005.08.018
- Revell, L. E., and Williamson, B. E. (2013). "Why are some reactions slower at higher temperatures?," *Journal of Chemical Education* 90(8), 1024-1027. DOI: 10.1021/ed400086w
- Saha, B., Iglesias, M., Dimming, I. W., and Streat, M. (2000). "Sorption of trace heavy metals by thiol containing chelating resins," *Solvent Extraction and Ion Exchange* 18(1), 133-167. DOI: 10.1080/07366290008934676
- Sajjadi, S.-A., Mohammadzadeh, A., Tran, H. N., Anastopoulos, I., Dotto, G. L., Lopičić, Z. R., Sivamani, S., Rahmani-Sani, A., Ivanets, A., and Hosseini-Bandegharai, A. (2018). "Efficient mercury removal from wastewater by pistachio wood waste-derived activated carbon prepared by chemical activation using a novel activating agent," *Journal of Environmental Management* 223, 1001-1009. DOI: 10.1016/j.jenvman.2018.06.077
- Saleh, T. A., Adio, S. O., Asif, M., and Dafalla, H. (2018). "Statistical analysis of phenols adsorption on diethylenetriamine-modified activated carbon," *Journal of Cleaner Production* 182, 960-968. DOI: 10.1016/j.jclepro.2018.01.242
- Seki, K., Saito, N., and Aoyama, M. (1997). "Removal of heavy metal ions from solutions by coniferous barks," *Wood Science and Technology*, 31(6), 441-447. DOI: 10.1007/BF00702566
- Sudha Rani, K., Srinivas, B., GouruNaidu, K., and Ramesh, K. V. (2018). "Removal of copper by adsorption on treated laterite," *Materials Today: Proceedings* 5(1), 463-469. DOI: 10.1016/j.matpr.2017.11.106
- Wei, W., Xu, B., and Huang, Q. (2016). "Controllable synthesis and catalytic property of novel copper oxides (CuO and Cu₂O) nanostructures," *International Journal of Materials Science and Applications* 5(1), 18-22. DOI: 10.11648/j.ijmsa.20160501.13
- Won, Y.-H., and Stanciu, L. A. (2012). "Cu₂O and Au/Cu₂O particles: Surface properties and applications in glucose sensing," *Sensors* 12(10), 13019-13033. DOI:

10.3390/s121013019

- Wu, M., Liu, H., and Yang, C. (2019). "Effects of pretreatment methods of wheat straw on adsorption of Cd(II) from waterlogged paddy soil," *International Journal of Environmental Research and Public Health*, 16(2). DOI: 10.3390/ijerph16020205
- Yang, K., Peng, J., Srinivasakannan, C., Zhang, L., Xia, H., and Duan, X. (2010). "Preparation of high surface area activated carbon from coconut shells using microwave heating," *Bioresource Technology* 101(15), 6163-6169. DOI: 10.1016/j.biortech.2010.03.001
- Yek, P. N. Y., Liew, R. K., Osman, M. S., Lee, C. L., Chuah, J. H., Park, Y.-K., and Lam, S. S. (2019). "Microwave steam activation, an innovative pyrolysis approach to convert waste palm shell into highly microporous activated carbon," *Journal of Environmental Management* 236, 245-253. DOI: 10.1016/j.jenvman.2019.01.010
- Zhou, Q., Li, X., Lin, Y., Yang, C., Tang, W., Wu, S., Li, D., and Lou, W. (2019). "Effects of copper ions on removal of nutrients from swine wastewater and on release of dissolved organic matter in duckweed systems," *Water Research*, 158, 171-181. DOI: 10.1016/j.watres.2019.04.036

Article submitted: October 14, 2019; Peer review completed: December 8, 2019; Revised version received: December 16, 2019; Accepted: December 17, 2019; Published: December 20, 2019.

DOI: 10.15376/biores.15.1.1112-1133